forests

MDPI

Article

Nonlinear Weather–Growth Relationships Suggest Disproportional Growth Changes of Norway Spruce in the Eastern Baltic Region

Roberts Matisons [1,*], Didzis Elferts [1,2], Oskars Krišāns [1], Volker Schneck [3], Holger Gärtner [4], Tomasz Wojda [5], Jan Kowalczyk [5] and Āris Jansons [1]

1 Latvian State Forest Research Institute 'Silava', 111 Rigas Str., LV-2169 Salaspils, Latvia; didzis.elferts@lu.lv (D.E.); oskars.krisans@silava.lv (O.K.); aris.jansons@silava.lv (Ā.J.)
2 Faculty of Biology, University of Latvia, Jelgavas Str. 1, LV-1010 Riga, Latvia
3 Thünen Institute of Forest Genetics, Eberswalder Chaussee 3a, D-15377 Waldsieversdorf, Germany; volker.schneck@thuenen.de
4 Swiss Federal Research Institute WSL, Zürcherstrasse 111, CH-8903 Birmensdorf, Switzerland; holger.gaertner@wsl.ch
5 Department of Silviculture and Genetics of Forest Trees, Forest Research Institute, Braci Leśnej 3, 05-090 Raszyn, Poland; T.Wojda@ibles.waw.pl (T.W.); J.Kowalczyk@ibles.waw.pl (J.K.)
* Correspondence: robism@inbox.lv; Tel.: +371-29789581

Abstract: Norway spruce (*Picea abies* (L.) H. Karst.) is predicted to decrease its abundance in the Eastern Baltic region as a result of climatic changes, and this process is already explicit at the southern limit of species lowland distribution. Still, there are uncertainties about the growth potential of Norway spruce within the region due to the plasticity of local populations. In this regard, an assessment of regional weather–growth responses, assuming a nonlinearity of the ecological relationship, can aid in the clarification of uncertainties regarding growth. Nonlinear regional weather–growth relationships for Norway spruce were assessed based on tree-ring widths from 22 stands spreading from Southern Finland to Northern Germany using dendrochronological methods and a generalized additive mixed model. Temporal and spatial stationarity of local linear weather–growth relationships was evaluated. Considering the drought sensitivity of Norway spruce, meteorological variables related to the summer moisture regime were the main predictors of radial increment, though conditions in winter and spring had complementary effects. Generally, the linear weather–growth relationships were spatially and temporary nonstationary, with some exceptions in Poland and Northern Germany. Explicit local specifics in the linear weather–growth relationships, which are common in the marginal parts of species' distribution, were observed in Estonia, Latvia, and Poland. The estimated regional weather–growth relationships were mostly nonlinear, implying disproportional responses to climatic changes, particularly to intensifying drought conditions across the studied climatic gradient. Still, the responses to winter temperature suggested that warming might contribute to growth. The estimated linear and nonlinear growth responses indicate strict limitation by drought conditions, implying reductions of increment due to climatic changes southward from Latvia, suggesting the necessity for proactive management. Nevertheless, in the northern part of the analyzed region, the projected climatic changes appear favorable for growth of Norway spruce in the near future.

Keywords: *Picea abies*; spatiotemporal climatic gradient; tree-ring width; phenotypic plasticity; regional analysis

Citation: Matisons, R.; Elferts, D.; Krišāns, O.; Schneck, V.; Gärtner, H.; Wojda, T.; Kowalczyk, J.; Jansons, Ā. Nonlinear Weather–Growth Relationships Suggest Disproportional Growth Changes of Norway Spruce in the Eastern Baltic Region. *Forests* **2021**, *12*, 661. https://doi.org/10.3390/f12060661

Academic Editor: Heli Peltola

Received: 29 April 2021
Accepted: 19 May 2021
Published: 22 May 2021

1. Introduction

Climatic changes are causing a northward shift of vegetation zones implying considerable changes in forests across vast areas [1]. Such shifts are resulting in substantial ecological and economic consequences [2]; hence, adaptive management is crucial for the sustainability of future forests [3–5]. For this, climate-smart selection of species/provenances

for the regeneration of stands has been highlighted as one of the most effective management practices [3,6]. Although assisted gene flow/migration has been advised [7], a high plasticity of local metapopulations of trees has also been observed [6,8–10], advocating conservative forest management, particularly under hemiboreal conditions [1,6]. Accordingly, comprehensive information on the sensitivity of trees to environmental fluctuations, such as weather conditions and shifting climate, is essential [11–13].

Radial increment of trees growing under seasonal climates has been widely applied for the assessment of tree sensitivity to short- and long-term environmental fluctuations (e.g., weather, climate) [13–16]. Tree-ring width (TRW) is the prevailing tree growth proxy due to its informativity, as well as convenient and time-efficient acquisition of data [16–19]. Retrospective analysis of various increment components derived from TRW provides detailed information on the sensitivity of trees to environmental fluctuations, aiding projections of tree performance in the future [16,20–22]. For this, linear weather–growth relationships have been widely used due to the simplicity and straightforwardness of modeling, which, however, can result in strongly biased extrapolations, particularly beyond the calibration ranges [14,23,24].

The ecological responses of quantitative traits across the environmental gradient are bell-shaped and, hence, nonlinear *per se*, though their plasticity (width and rigidity) can vary among species, populations, and genotypes [11,14,25–27]. Accordingly, close-to-linear responses can be observed only in distinct parts of a gradient [14]. A temporal shift of the environmental gradient, as in the case of climatic changes, is likely to result in the nonstationarity of the local linear responses [14,23,24,28,29], implying that they are often outdated [14,30]. A generalization of responses accounting for their nonlinearity across substantial parts of the spatiotemporal climatic gradient(s) is therefore essential for more reliable predictions [12,22,26,27]. Analysis of the climatic rather than spatial gradient provides better insight into the growth responses of trees under a changing climate (shifting climatic gradient) [11,25,27,31]. Such studies agree on predicting disproportional and/or heterogeneous responses to a changing climate across regional climatic gradients [12–14,22,32]. This highlights the relevance of extensive regional-scale analysis [8,12,13,25].

As long-lived organisms, trees have evolved high phenotypical plasticity, allowing them to survive the highly temporal variability of weather conditions [7,33]. Nevertheless, tree populations have often specialized to certain local conditions, genetically restraining their plasticity, irrespective of high gene flow [30,33–35]. This presumes the existence of local population-wise optimum conditions. Accordingly, climatic changes are subjecting trees to 'novel', sometimes even extreme conditions, testing their phenotypic plasticity [7,12,36], thus highlighting the necessity for proactive management to ensure forest sustainability [3,5,33].

Genetic (local) specialization implies an uneven adaptability of metapopulations (provenances) to certain weather conditions and their changes [30,33,36], diversifying responses to large-scale environmental fluctuations [8,12,13,25] and mitigating the expression of common limiting factor(s) [14]. The sensitivity of tree growth to weather conditions is also affected by aging due to morphological and physiological tradeoffs [28,37,38]. Furthermore, weather conditions can have a direct as well as legacy effect on wood formation [39,40], modulating growth responses [12], hence adding complexity to the weather–growth interactions [8,41]. However, marginal conditions, as on the margin of a species' range, can override the genetic specialization of metapopulations [36]. Accordingly, information about the tolerance and adaptability of populations of trees is crucial for growth modeling and sustainable proactive management [6,13,31,42].

Norway spruce (*Picea abies* (L.) H. Karst.) is an economically important species in the Eastern Baltic region [43–45], yet its abundance is predicted to decrease due to intensifying shortage of water in summer [1,5]. Due to high sensitivity to drought and its legacy effects (e.g., pest outbreaks; [46–48]), commercial application of Norway spruce in Central and Western Europe is being reduced, favoring more sustainable alternatives [6,44,49]. However, in the Eastern Baltic region, which includes the current southern lowland distribution

limit of Norway spruce [36,50], diverse weather–growth responses have been observed on regional and local scales [51,52], increasing the uncertainties regarding the growth potential of the species [4,5,43,51]. Accordingly, comprehensive analyses generalizing responses to weather fluctuations across the regional climatic gradient including the southern distribution limit of the species [36] can aid in the reduction of such uncertainties [51,52]. The aim of the study is to assess responses of maturing Eastern Baltic Norway spruce to weather fluctuations across the regional climatic gradient. We hypothesized that the sensitivity of increment of Norway spruce to weather factors related to water deficit in summer intensifies southward, yet a regional response might indicate a threshold value. However, we assumed that the expression of regional responses might be mediated by local specialization of metapopulations.

2. Materials and Methods

2.1. Study Sites, Sampling, and Measurements

To assess the plasticity of radial increment of Norway spruce in response to interannual weather fluctuations across the regional Eastern Baltic climatic gradient, 22 sites (forest stands > 1.5 ha in area) distributed from Southern Finland to Northern Germany were sampled (Figure 1). The stands represented six localities distributed 400–600 km apart along a transect representing hemiboreal and nemoral conditions. To account for local specialization of tree metapopulations [8,53], in each location, three to six stands were sampled. The stands were growing under lowland (elevation < 250 m a.s.l.) mesotrophic conditions on dry sandy or silty podzolic soils (Table 1). The topography of sites was flat, and the stands were naturally regenerated (planted in Northern Germany), closed canopy, and conveniently managed. Most of the stands had an admixture of birch (*Betula* spp. L.) and/or pine (*Pinus sylvestris* L.). The age of the stands ranged from 71 to 120 years (with the mean of 98), corresponding to maturing and mature stands in Northern Europe.

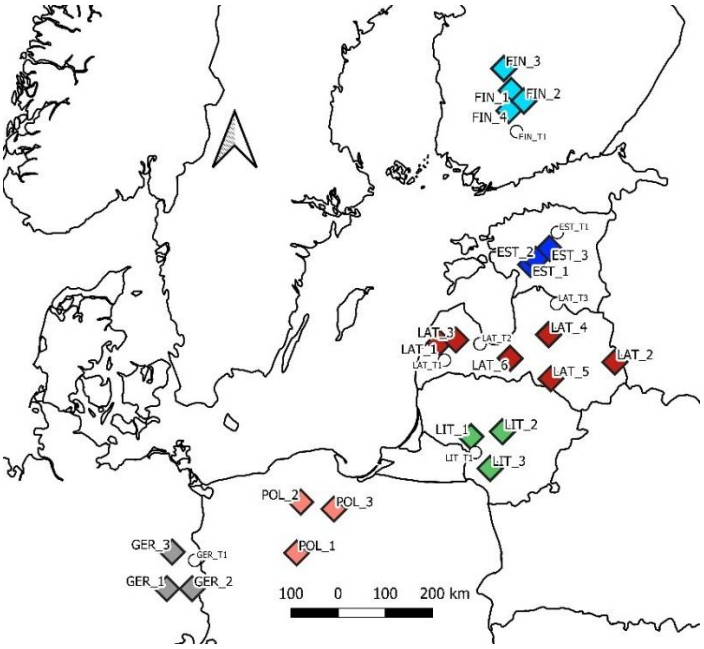

Figure 1. Locations of the sampled stands of Norway spruce used for assessment of linear weather–growth relationships and calibration of model (squares). Circles denote stands used for model verification. Arrow represents geographic north.

Table 1. Location, soil type, composition (admixture), and age of the sampled stands of Norway spruce.

Site	Latitude, ° N	Longitude, ° E	Soil	Admixture	Stand Age
FIN_1	61.81	24.31	Silty	Pine, 20%	95
FIN_2	61.61	24.81	Silty	Pine, 10%	101
FIN_3	62.23	24.01	Sandy		121
FIN_4	61.43	24.21	Silty		99
EST_1	58.49	24.98	Silty	Pine, 10%	92
EST_2	58.59	25.18	Sandy	Pine, 20%	101
EST_3	58.79	25.69	Silty	Birch, 30%	121
LAT_1	56.99	21.76	Silty	Pine, birch, 30%	108
LAT_2	56.58	27.85	Sandy	Pine, 10%	79
LAT_3	57.05	22.33	Silty	Birch, 30%	112
LAT_4	57.15	25.58	Silty		97
LAT_5	56.31	25.62	Sandy	Birch, 10%	110
LAT_6	56.71	24.23	Silty		111
LIT_1	55.21	22.91	Silty		75
LIT_2	55.31	23.96	Sandy	Pine, 20%	91
LIT_3	54.61	23.56	Sandy	Birch, pine, 30%	85
POL_1	52.82	17.47	Silty		82
POL_2	53.79	17.46	Sandy	Pine, 20%	112
POL_3	53.71	18.54	Silty	Birch, 10%	108
GER_1	51.86	13.60	Silty		83
GER_2	51.92	14.37	Silty	Birch, 10%	72
GER_3	52.56	13.60	Silty		79

The sampled stands represented the regional climatic gradient ranging from temperate oceanic in Northern Germany and Poland to cold humid continental in Southern Finland and the Baltic States. The sites were mostly located in coastal areas (Figure 1). In 1989–2018, the mean annual temperature ranged from 4.2 to 10.2 °C at sites in Southern Finland and Northern Germany, respectively (Table 2). July and January were the warmest and coldest months, respectively, though interannually, the winter temperature regime was more variable compared to summer [54]. The mean annual precipitation sums were generally similar for sites ranging 535–772 mm in Finland and Latvia, respectively, though considering differences in temperature, they resulted in different levels of summer soil water deficit [55]. Studied sites showed similar annual distribution of precipitation, with the highest monthly values occurring during the vegetation period, which extends from April to October (particularly in July and August), which accounts for approximately half of the annual precipitation (Table 2). Warming, particularly during the dormant period, and extension of the vegetation period are the main manifestations of global climatic changes in the studied region in recent decades, though the amount of annual precipitation expresses a negative trend in Poland and Germany [56].

In each stand, increment cores were collected from 20–30 visually healthy, not tilting trees using a 5 mm increment corer. Two cores per tree from randomly oriented, yet opposite sides of stem at 1.3 m height were taken. In total, 585 trees were sampled during the dormant periods of 2017 and 2018. In the laboratory, cores were fixed on wooden mounts, and their surface was leveled for measurements of TRW using the WSL core microtome [57], or alternatively by progressive grinding. A LINTAB 5 measurement table (RinnTech, Heidelberg, Germany) was used to manually measure TRW to the nearest 0.01 mm.

Table 2. Climatic description of the studied sites by country (the ranges are given). Data represent the 1989–2018 period. January and July are the coldest and warmest months, respectively. The May–September period generally corresponds to the vegetation period. Number in brackets indicate number of sampling sites. St. dev.—standard deviation.

	FIN (4)	EST (3)	LAT (6)	LIT (3)	POL (3)	GER (3)
Mean annual temperature, °C	4.2–4.7	6.2–6.7	6.1–7.4	7.5–7.6	8.4–9.2	9.8–10.2
Annual temperature st. dev, °C	0.73–0.74	0.68–0.69	0.64–0.67	0.65–0.66	0.7–0.73	0.71–0.72
Mean minimum January temperature, °C	−19.9–−19.3	−16.2–−15.2	−15.3–−10.1	−12–−11.2	−7.9–−7.5	−6.5–−6.1
Mean maximum January temperature, °C	1.9–2.4	4.1–4.5	3.9–5.1	5.3–5.7	8.2–9	10.2–10.4
Mean minimum July temperature, °C	11.5–12.1	13.0–13.7	12.5–13.7	13.2–13.4	13.3–13.8	14.1–14.4
Mean maximum July temperature, °C	22.1–22.6	22.6–22.8	21.4–23.6	23.6–23.8	22.6–24.4	24.5–25.3
Mean minimum May–September temperature, °C	7.9–8.5	9.7–10.5	9.4–10.8	10.5–10.7	10.8–11.2	11.8–12.1
Mean maximum May–September temperature, °C	18.1–18.6	19.2–19.3	18.6–20.5	20.7–20.9	20.1–21.7	22–22.8
Mean annual precipitation, mm	538–587	696–699	641–772	631–696	535–646	551–585
Annual precipitation st. dev., mm	59–66	82–84	75–91	71–78	71–81	75–79
Mean May–September precipitation, mm	291–310	324–336	310–356	328–344	296–338	284–297
May–September precipitation st. dev., mm	56–61	63–69	59–71	64–67	62–70	62–66

2.2. Data Analysis

Visual and statistical crossdating was performed to ensure the quality and correct dating of the time series of TRW. For description of the high-frequency variation of TRW, first-order (lag-1) autocorrelation, mean sensitivity, mean interseries correlation (r-bar), expressed population signal (EPS), and signal to noise ratio (SNR) were calculated based on detrended time series [58,59]. A residual chronology was produced for each stand to assess the high frequency of TRW [12,58]. Individual time series were double detrended by a negative exponential curve and by a flexible cubic spline with the rigidity of 2/3 of series length and 50% frequency cutoff to remove the effects of aging and disturbances, respectively [58]. The detrended individual time series were prewhitened using an autoregressive model ('ar1') to omit the effects of previous growth [60] and averaged into stand chronologies via the biweight robust means [58]. Chronologies for the common period of 1954–2017, when the EPS for 30-year time windows exceeded 0.85 (cf. [59]), were used for analysis.

Considering that the individual stands represent only a limited part of the regional climatic gradient [14,27,61], local weather–growth relationships were assessed via bootstrapped Pearson correlation analysis (nonparametric percentile interval bootstrapping with replication; 1000 iterations) between the residual chronologies and local weather variables. To assess temporal stability (stationarity) of the linear weather–growth relationships, bootstrapped correlation analysis was performed for 30-year moving time windows (with one-year lags; [62]). Mean monthly temperature, precipitation sum, and the standardized precipitation evapotranspiration index (SPEI, calculated with respect to the preceding three months; [63]) were used as weather variables. Weather variables were arranged into time windows from June in the year preceding tree-ring formation (previous June) to October in the year of tree-ring formation, thus accounting for carryover effects [40,64]. Gridded climatic data (CRU TS) were used [54]; grid points were located $\leq$ 40 km from the studied stands.

A generalized additive mixed model [65] was used to assess main regional responses of the relative additional radial increment (indices of residual chronologies) to weather variables across the spatiotemporal climatic gradient, and their plasticity (nonlinearity). Such a model allows an estimation of responses according to the shifting baseline of the independent variable(s). Previous studies have shown such an approach to be efficient for the analysis of heterogeneric ecological data representing spatiotemporal gradients (e.g., tree-ring networks) [11,12,25,27]. The indices of the residual chronologies were used as the response variable. As the predictors, diverse combinations of meteorological values, as hinted by the correlation analysis, were tested. As bell-shaped responses were expected, the basis dimension of the smoothing terms was restricted to four, which corresponds to a curve with up to three inflection points, thus avoiding overfit. The interactions between the predictors (numerical) were not tested due to limitations set by the amount of data.

To account for the hierarchical structure of tree-ring data, dependencies arising from phenotypical plasticity and local specialization of metapopulations, as well as differences in phenology [17,18,30], year, and site, were included in the model as nested random effects. Tree age was included in the models accounting for the temporal correlation (ρ) arising from the aging of trees [24,38]. A restricted maximum likelihood approach was used to fit the models. Smoothing parameters were estimated via the generalized crossvalidation procedure. Regression spline with shrinkage was used to smoothen the results. The best-performing set of meteorological variables (according to the arbitrary selection principle) was selected based on the Akaike information criterion (AIC). Normality and homogeneity of model residuals were checked by diagnostic plots. The variance inflation factor was used to assess the collinearity of the predictors; collinear variables (with the criterion > 5) were excluded from the model. The lack of overfit of the refined model was verified by crossvalidation based on an independent tree-ring dataset (not used in calibration) representing sites across the studied locations (Supplementary Material, Table S1). Data analysis was performed in R (v. 4.0.3; [66]), using the packages 'mgcv' [65], 'dplR' [58], 'car' [67], and 'bootRes' [62].

3. Results

3.1. Local Weather–Growth Correlations

Most of the time series (≥80% per stand) showed good agreement, as indicated by EPS, r-bar, and SNR (Table 3), and were used for the analysis. In total, TRW series from 537 trees were crossdated (16 to 30 trees per stand, Supplementary Material, Figure S1), and the EPS values for all stands well exceeded 0.85 (cf. [59]). During the common period of 1954–2017, the agreement of high-frequency variation of TRW among trees within a stand (r-bar $\geq$ 0.34, mean = 0.47) and strength of the environmental signal (SNR $\geq$ 8.71, mean = 18.92) were high (Table 3). Nevertheless, the agreement among trees, as indicated by r-bar and SNR, as well as the mean sensitivity and the mean values of TRW (Supplementary Material, Figures S2 and S3), increased southward. In contrast, first-order autocorrelation, which was high, tended to increase northward (ranging from 0.61 to 0.78 in Northern Germany and Southern Finland, respectively), suggesting a stronger dependence of TRW on previous growth under colder climates (Table 2).

During the analyzed period, correlations between TRW and meteorological variables showed an explicit continuous geographic gradient as the significance of the variables related to winter temperature and summer precipitation regime switched (Figure 2). Nevertheless, some local specifics were found. In Southern Finland, TRW mainly correlated with temperature (positively) and precipitation (negatively) in spring. In some sites, though, TRW correlated positively with SPEI and negatively with temperature in summer. In Estonia and Latvia, the relationships between TRW and meteorological variables showed local specifics, as indicated by a higher number yet lower frequency of significant correlations. Nevertheless, TRW mainly correlated with temperature and precipitation regime (SPEI) during the dormant period (December and February; positive), as well as with summer precipitation (positive) and temperature (negative).

Under the warmer climate in Lithuania, TRW of spruce showed positive common correlations with precipitation and SPEI during the May–July period, yet temperature in June and in the previous September was significant in single stands (Figure 2). In sites in Poland and Northern Germany, factors related to moisture regime throughout the vegetation period showed common correlations with TRW. Temperature in June and in the previous September showed frequent negative correlations in most of the stands, particularly in Northern Germany. Additionally, common positive correlations with precipitation in February were found.

Table 3. General statistics for the datasets of crossdated tree-ring width time series of the stands of Norway spruce from the Eastern Baltic region for the 1954–2017 period. SENS—mean sensitivity, AC1—first-order autocorrelation, N—number of crossdated time series, r-bar—mean interseries correlation, EPS—expressed population signal, SNR—signal to noise ratio.

Site	Timespan	Mean ± St. Dev, mm	SENS	AC1	N	r-Bar	EPS	SNR
FIN_1	1923–2017	2.16 ± 0.79	0.17	0.76	30	0.44	0.94	15.50
FIN_2	1917–2017	1.88 ± 0.71	0.16	0.81	22	0.36	0.90	8.71
FIN_3	1897–2017	1.52 ± 0.54	0.18	0.75	28	0.34	0.91	10.08
FIN_4	1919–2017	1.50 ± 0.66	0.19	0.81	26	0.39	0.93	13.87
EST_1	1927–2018	1.95 ± 0.80	0.20	0.78	30	0.51	0.96	22.75
EST_2	1918–2018	2.02 ± 0.73	0.20	0.68	25	0.35	0.91	10.32
EST_3	1898–2018	1.69 ± 0.68	0.20	0.73	28	0.44	0.94	14.82
LAT_1	1900–2017	1.46 ± 0.76	0.24	0.77	20	0.54	0.96	21.79
LAT_2	1931–2017	2.80 ± 1.53	0.27	0.73	18	0.43	0.92	11.70
LAT_3	1900–2017	1.21 ± 0.47	0.20	0.73	19	0.39	0.91	10.35
LAT_4	1913–2017	2.26 ± 1.45	0.21	0.86	20	0.60	0.96	26.92
LAT_5	1900–2017	2.07 ± 0.87	0.24	0.65	19	0.40	0.91	10.29
LAT_6	1900–2017	1.56 ± 0.79	0.22	0.80	24	0.57	0.96	27.15
LIT_1	1933–2017	2.15 ± 1.02	0.23	0.76	27	0.49	0.96	22.57
LIT_2	1935–2017	2.35 ± 1.15	0.21	0.79	27	0.53	0.96	24.85
LIT_3	1943–2017	2.73 ± 1.15	0.22	0.74	28	0.46	0.95	20.53
POL_1	1937–2018	1.73 ± 0.82	0.26	0.71	29	0.63	0.98	43.57
POL_2	1907–2018	1.72 ± 0.93	0.31	0.66	26	0.49	0.96	23.65
POL_3	1911–2018	2.16 ± 1.04	0.27	0.70	28	0.41	0.94	14.90
GER_1	1935–2017	3.19 ± 1.44	0.32	0.55	29	0.58	0.96	23.97
GER_2	1946–2017	2.42 ± 1.23	0.30	0.65	18	0.51	0.95	17.61
GER_3	1939–2017	1.79 ± 0.97	0.34	0.64	16	0.58	0.95	20.35

3.2. Nonstationarity of Local Correlations

Temporal shifts of the correlations revealed the nonstationarity of the local linear weather–growth relationships across the studied climatic gradient (Supplementary Material, Figures S4–S9). Under the colder climate in Southern Finland, the correlations with temperature in May lost significance during the early part of the analyzed period (Supplementary Material, Figure S4). Concomitantly, the effect of temperature in April intensified locally, suggesting shifts in the period of responsiveness of trees. The negative correlation with temperature in June was significant during the mid-part of the analyzed period or intensified, and the effect of summer precipitation tended to increase.

In Estonia, the nonstationarities in weather–growth relationships were mainly expressed as a strengthening of positive correlations with summer precipitation (Supplementary Material, Figure S5). Shifts in tree sensitivity to temperature earlier in spring (from May to April) or summer temperature occurred locally. In Latvia, the shifts in correlations were local, though the effects of summer temperature and precipitation intensified during the second part of the studied period (Supplementary Material, Figure S6). Correlations with temperature in January and February lost their significance during the early part of the analyzed period, while the effect of December temperature was intensifying in the most recent intervals.

In Lithuania, where the effect of the water regime in summer on TRW was prevailing (Figure 2), the nonstationarities in weather–growth correlations were related to summer precipitation (Supplementary Material, Figure S7). Intensifications of correlation with June precipitation and SPEI, or a switch of the effects of June SPEI and precipitation of the previous July, occurred (LIT_3 site). At the southern margin of lowland distribution of Norway spruce in Poland, the shifts in climate–growth correlations appeared to be complex and local (Supplementary Material, Figure S8). The negative correlations with temperature in June and July intensified and became significant at the later part of the analyzed period, yet the effects of February precipitation and July SPEI weakened. Still,

some highly stationary correlations (June SPEI) were estimated. Both intensification and weakening of correlation with temperature in the previous September occurred locally.

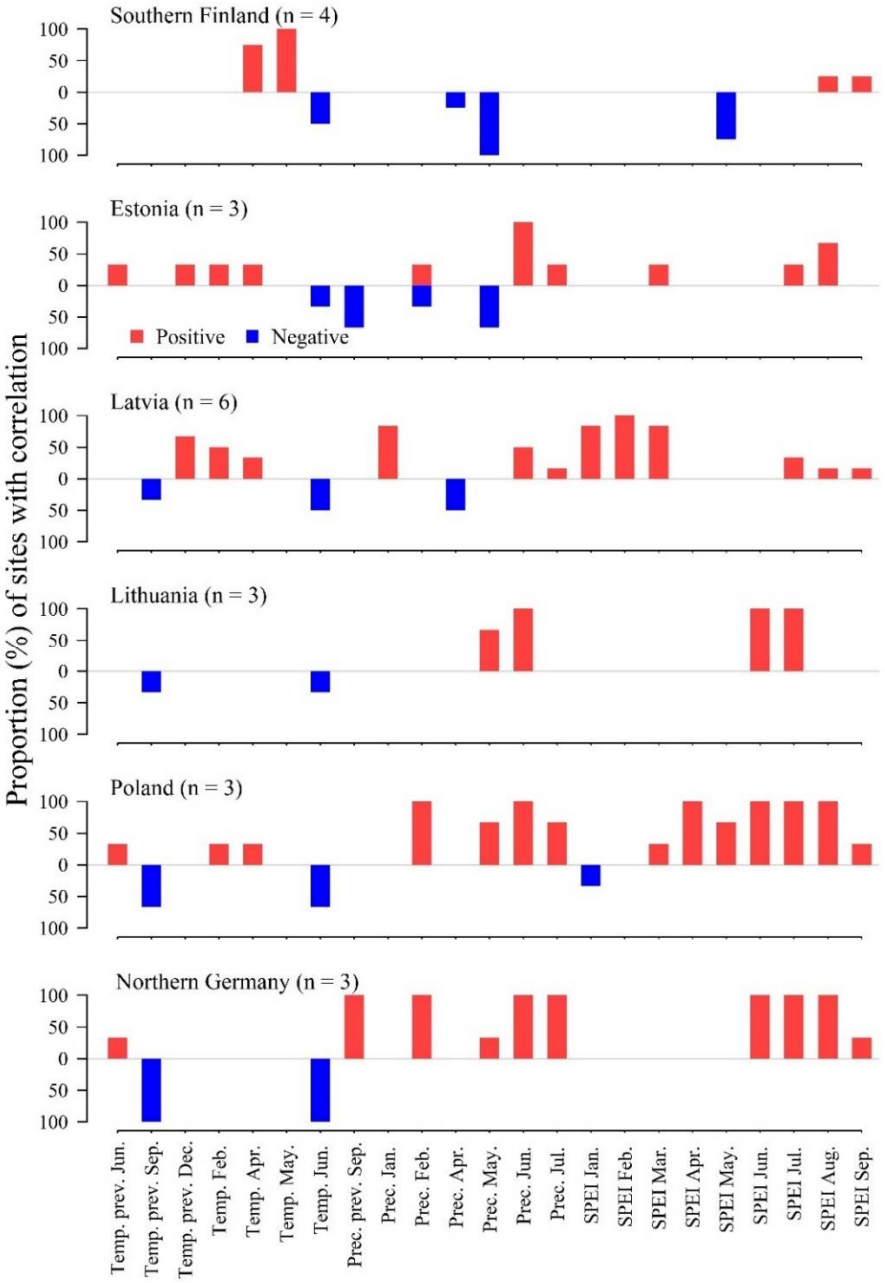

Figure 2. The proportion of stands of Norway spruce showing significant (p-value < 0.05) Pearson correlation coefficients between the residual chronologies of tree-ring width and meteorological variables: monthly mean temperature (Temp.), precipitation sums (Prec.), and standardized precipitation evapotranspiration index (SPEI) by countries. The bars below zero represent the negative correlations. The analysis was conducted for the 1954–2017 period. Only the meteorological variables showing significant correlations are shown.

In Northern Germany, both stationary and nonstationary correlations were estimated (Supplementary Material, Figure S9). A clear limiting effect of SPEI in July was indicated by prevailingly stationary correlations. The correlations between TRW and temperature in June and July were found to be weakening and/or lost significance. The correlations with temperature in the previous September became significant at the later part of the analyzed period.

3.3. Regional Weather–Growth Response Curves

Nonlinear responses of TRW of Eastern Baltic Norway spruce to meteorological variables across the regional spatiotemporal climatic gradient were identified by the generalized additive mixed model. The estimated response curves (Figure 3) revealed the linkage between local climates and weather–growth responses. The refined model was significant (p-value < 0.001) and contained 5 of the 51 meteorological variables tested (Table 4). The adjusted R^2 for the fixed part of the model was intermediate (0.185; cf. [12]), implying the effect of local specialization. The conditional, though, pseudo-R^2 of the model was intermediate (0.48), indicating lack of overfit. The crossvalidation of the refined model based on an independent dataset confirmed the lack of overfit, as the root mean square errors calculated for the calibration and verification datasets were comparable (0.162 and 0.165, respectively).

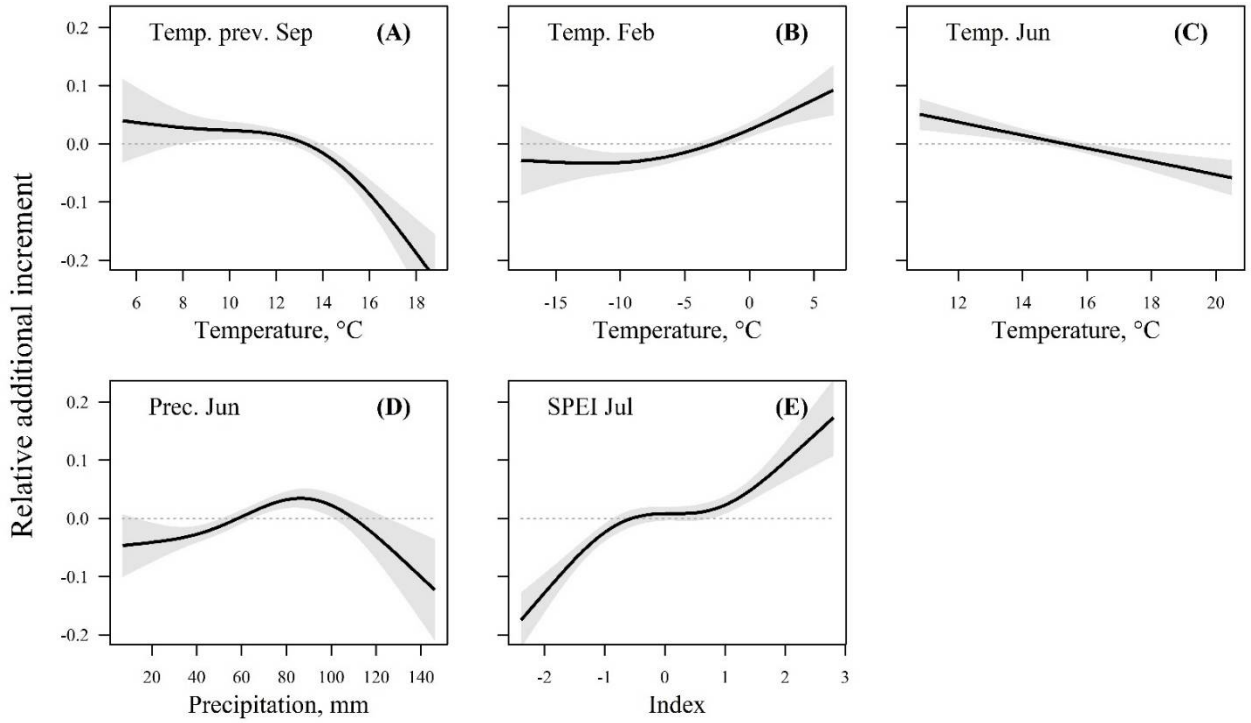

Figure 3. The estimated approximate smoothing splines (dashed lines denote 95% confidence intervals) of the responses of relative additional radial increment (tree-ring width index) of Eastern Baltic Norway spruce to meteorological variables (monthly mean temperature in previous September (**A**), February (**B**), and June (**C**), precipitation sum in June (**D**), and standardized precipitation evapotranspiration index SPEI in July (**E**)) across the regional climatic gradient in 1954–2017.

The meteorological variables included in the refined model were strictly significant (p-value $\leq$ 0.001, F-value $\geq$ 7.6), and their effective degrees of freedom ranged from 1.00 to 2.87, which were below the limit set for the basis dimensions (four). This implied ecologically sound response curves with up to two inflection points. The effect of tree age on growth responses was low, as indicated by the correlation term (ρ = 0.16), likely due to most of the trees being in the maturing phase during the analyzed period. Regarding the random effects, year had approximately four times higher variance compared to site, indicating that phenotypic plasticity exceeded local specialization of the studied metapopulations of Norway spruce.

Table 4. Statistics of smoothing splines of the generalized additive mixed model of the relationships between the relative additional radial increment (tree-ring index) of Norway spruce from the Eastern Baltic region and meteorological variables: month mean temperature, precipitation, and precipitation evapotranspiration index (SPEI) during the 1954–2017 period.

Fixed Effects			
Smoothening Term	**Effective Degree of Freedom**	***F*-Value**	***p*-Value**
Previous September temperature	2.72	18.9	<0.001
February temperature	2.22	14.2	<0.001
June temperature	1.00	15.4	<0.001
June precipitation	2.80	7.6	<0.001
July SPEI	2.87	26.8	<0.001
Random Effects			
Term	Variance		
Year	0.0162		
Stand	0.0039		
Residual (scale)	0.0155		

The refined model included a subset of the meteorological variables (Table 4) highlighted by the site-level correlation analysis (Figure 2, Figures S4–S9). Though at the regional scale, the responses to them were mostly nonlinear (Figure 3), indicating the biasness of the linear response across a wide spatiotemporal climatic gradient. Among the selected meteorological variables, SPEI in July, which represents moisture balance in summer, had the strongest effect (highest *F*-value) on relative additive increment of Norway spruce (Table 4) at the regional scale. The response to July SPEI was generally positive (Figure 3E), with an explicit reaction to severe drought conditions, yet a slightly milder reaction to abundant precipitation. An interval of irresponsiveness was estimated when SPEI ranged circa −0.8–0.6, which corresponds to a balanced moisture regime.

The response of TRW to June temperature, which was estimated with nonstationary local correlations (Supplementary Material, Figures S4–S9), was linear and negative across the regional climatic gradient (Figure 3C). However, the fluctuations of June temperature within the studied range accounted for relatively small changes of relative additional increment. The effect of June precipitation was weaker (Table 4), and the nonlinear response curve showed an optimum range of circa 70–100 mm month^{-1}, which resulted in a positive additional increment (Figure 3D).

Temperature in the previous September, which was estimated with the second strongest effect on TRW at regional scale (Table 4), indicated carryover effects of weather fluctuations. The response curve indicated a threshold value of circa 13 °C, exceeding which, a rapid reduction of increment occurred (Figure 3A). Considering the location of the studied stands in temperate climate zone, the temperature in winter (February) also had a significant effect on increment (Table 4). The response of increment to it also indicated a threshold value of circa −6 °C; however, exceeding it, a positive reaction was estimated (Figure 3B).

4. Discussion

4.1. Plasticity and Stationarity of Weather–Growth Relationships

Spatiotemporal shifts in the linear weather–growth correlations (Figure 2 and Figures S4–S9) and the estimated response curves (Figure 3) highlighted the plasticity and nonlinearity of weather–growth relationships [14,19,25] of Norway spruce in the Eastern Baltic region. The plasticity of responses is indicative of both regional specialization [17,18,26,31,35] and adaptability to changing conditions [30,34,68]. Within the studied region, which included the southern margin of lowland distribution of spruce [36,50], phenotypical plasticity exceeded genetic specialization of weather–growth sensitivity (Table 4), implying some adaptability of populations in the medium term [4,18,30,42,68]. The local genetic specialization, however, was weaker compared to that of Scots pine from the same localities [11],

likely due to the common sensitivity of Norway spruce to water shortage [52] and its legacy effects [46]. Still, local specialization has likely mediated regional growth responses [13], as suggested by the locally specific correlations (Figure 2), thus supporting the hypothesis. The interaction between environmental factors [8,23,36,41] can also contribute to the nonstationarity of weather–growth responses at regional level.

Near the distribution limit, site factors and adaptation to them are crucial for the survival of trees, resulting in locally specific growth sensitivity, yet in the core areas, trees adapt to 'common' fluctuations to maximize growth and competitiveness [12,36]. Accordingly, relaxation of common limiting factors can be indicative of conditions comparable to distribution margins. Local specifics of weather–growth correlations were explicit in Estonia and Latvia (Figure 2, Figures S5 and S6), suggesting that the 'natural' range of Norway spruce might have already shifted northward [1]. This is supported by the fact that Norway spruce has suffered diebacks and is already struggling to survive in Poland and Germany [36,46]. Alternatively, this might be explained by the distribution of Eastern Baltic metapopulation(s) of Norway spruce [69]. Local specifics in the shifts in linear relationships were found in Poland (Supplementary Material, Figure S8), which occur on the 'current' southern distribution limit [50]. Accordingly, this highlights spatial nonstationarity (heterogeneity) of weather–growth correlations caused by species' range shifts [4,14,29,70].

The weather–growth relationships are affected by size-dependent physiological processes [24,37,38,40] and the intensity of the weather conditions [13,29,71]. Accordingly, aging and climatic changes are the concomitant causes of temporal nonstationarities of weather–growth correlations [14]. The age effect estimated by the refined model was low (ρ = 0.16), which can be explained by the studied trees being in the maturing phase, when the within-tree water relations are generally balanced [24,37]. The low age effect implied that the observed nonstationarities of the local linear weather–growth relationships (Figure 2 and Figures S4–S9) arose from warming and increasing variability of summer precipitation [56] rather than aging [28,37,38]. Accordingly, the estimated regional curves (Figure 3) imply the presence of stationary, yet nonlinear regional weather–growth relationships [14], generalizing responses under moderate to marginal conditions [12,61]. Such responses also imply disproportional effects of climatic changes [14,32,61,70], particularly in the contracting parts of species' range and shifting conditions [12,13,36].

The stationarity (stability) of weather–growth relationships is crucial for the reliability of reconstructions of past environments, as well as projections of future growth [12,26,27,72,73], while the nonstationarities of linear relationships are one of the main causes for the divergence problem [23,72,74]. The observed nonlinear regional weather–growth responses (Figure 3) indicate that the nonstationarities (both temporal and spatial) of local linear weather–growth relationships (Figure 2 and Figures S4–S9) were largely caused by the shifts in the regional climatic gradient [12,13] and are hence expected [14]. Accordingly, only linear weather relationships which appear stationary across wide climatic gradients should be used for reconstructions [14,73]. Alternatively, application of nonlinear weather–growth relations accounting for the modulating effects of climate [11,27] could reduce the bias and the divergence problem during reconstruction/projections. This highlights the importance of large-scale analysis of growth responses for evaluating the spatiotemporal stationarity of responses [8,11,14,19].

4.2. Regional Growth Responses

As hypothesized, weather variables related to the moisture regime and hence water deficit in summer had the strongest effect on relative radial additional increment of Eastern Baltic Norway spruce (Figures 2 and 3, Table 4). Such effects were also observed in the northern part of the analyzed region in Southern Finland (Figure 2), likely as a consequence of climatic change (warming) [13,27,29], thus verifying the presence of regional drivers of growth [12,13,27,52]. In the studied region, July is the warmest month (Table 2), when intense assimilation [75–77] and evapotranspiration [29,55] occur, boosting demand for water; hence, SPEI had an explicit effect on increment (Figure 3E, Table 4). Although late-

wood, which comprises the smaller part of TRW, is formed in July in most sites [15,40,76], SPEI is cumulative and accounts for the legacy of the preceding months [63], explaining the explicit effect on increment. Moisture balance in July can also affect further lignification of xylem by altering assimilation [15,40,75,76].

The linear negative response to June temperature (Figure 3C) implied a direct stationary effect of increased evapotranspiration [55] and hence water deficit on assimilation [15,76,78], though the local responses were sometimes contrasting (Supplementary Material, Figures S4–S9), probably due to interaction between precipitation and temperature regimes [56]. The bell-shaped response to precipitation in June (Figure 3D) suggested tradeoffs between sufficient water supply needed for assimilation and cell expansion [15,40,75,76,78], and, likely, reduced assimilation due to cloudiness [79]. Likewise, negative local responses to precipitation in May were observed under the cooler climate in the northern part of the studied region (Figure 2). Such a response presumes differing effects of abundant summer precipitation under nemoral and hemiboreal conditions [8,25,29,80], implying complex effects of the drought-related weather conditions across the regional climatic gradient.

The responses of increment to conditions preceding xylogenesis (Figures 2 and 3) highlighted the relevance of carryover effects of weather fluctuations [27,40,60,64] at a regional scale. The effect of temperature in the previous September (Figure 3A), which had the second strongest effect on increment (Table 4), could be explained by the tradeoffs between reproduction and growth [81]. Norway spruce is a masting species, and formation of primordia of generative buds is triggered by increased temperature at the end of the growing period [82], implying an allocation of assimilates for reproduction in the following year rather than growth [81]. Apparently, masting was triggered by mean September temperature exceeding 13 °C, and the effect was multiplicative (Figure 3A). The estimated response curve also indicated that this effect intensified under warmer climates (southward), likely as an evolutionary adaptation promoting genetic specialization toward the distribution limit [12,35,61].

Considering the cold tolerance of Norway spruce and location of the studied stands under temperate climates (Table 2), meteorological conditions in winter (Figures 2 and 3) had moderate (Table 4), yet complementary effects [26,53]. Such effects, though, were explicit at the regional scale, implying the relevance of large-scale analysis. The responses to temperature in February indicated that low temperatures (ranging from −12 to −5 °C) caused slight negative additional increment (Figure 3B), likely due to cold damage [83], particularly to the root system [84,85]. Additionally, such monthly mean temperature can indicate the occurrence of thaws, which are becoming more frequent [56] and reduce the cold hardiness of trees [86,87]. Temperatures above circa −3 °C resulted in positive additional increment, likely due to improved overwintering [83].

Positive local linear effects of precipitation in winter months were found in Estonia, Latvia, and particularly in Poland and Northern Germany (Figure 2). Under cooler climates (Latvia and Estonia), such effects might be related to the positive insulating effects of snow cover on roots and, hence, water relations in the following season [84]. However, the absence of such an effect in Southern Finland (Figure 2) might probably be explained by the more stable snow conditions. Under warmer climates (Poland and Germany), where snow cover is occasional [56], the effect of winter precipitation might be related to the restoration of water table and, thus, water availability in the subsequent vegetation period [88]. Such dual effects likely blurred regional responses to winter precipitation [13].

5. Conclusions

Regional-scale analysis highlighted the nonlinear responses of relative additional radial increment to weather conditions associated with drought across the spatiotemporal climatic gradient of the Eastern Baltic region, though the effects were complex. Meteorological conditions in winter had complementary effects, adding complexity to regional weather–growth relationships. Explicit local genetic specialization, which is typical for

metapopulations of trees growing near their distribution margins, was indicated by locally specific weather growth relationships in Estonia and Latvia, as well as in Poland, implying an ongoing northward shift of the Norway spruce range. Nevertheless, the estimated local specialization, and hence the genetic control of growth responses, suggests potential for breeding of more tolerant genotypes for application in the Baltic States through supplementation of breeding populations with southern provenances.

Supplementary Materials: The following are available online at https://www.mdpi.com/article/10.3390/f12060661/s1, Table S1, General statistics of the datasets of crossdated tree-ring width time series of the open-pollinated stands of Norway spruce from the Eastern Baltic region for the 1954–2017 period used for crossvalidation of the refined nonlinear model. SENS—mean sensitivity, AC1—first-order autocorrelation, N—number of crossdated time series, r-bar—mean interseries correlation, EPS—expressed population signal, SNR—signal to noise ratio; Figure S1, Replication of the crossdated tree-ring width time series of the Eastern Baltic open-pollinated Norway spruce from the studied mesotrophic well-drained managed stands from Southern Finland through Northern Germany; Figure S2, Mean time series of crossdated tree-ring width of the Eastern Baltic open-pollinated Norway spruce from the studied mesotrophic well-drained managed stands from Southern Finland through Northern Germany; Figure S3, Residual chronologies of crossdated tree-ring width of the Eastern Baltic open-pollinated Norway spruce from the studied mesotrophic well-drained managed stands from Southern Finland through Northern Germany for the 1954–2017 period. The mean interseries correlation is shown in each panel; Figure S4, Bootstrapped Pearson correlation coefficients between residual chronologies of tree-ring width of the studied open-pollinated stands of Norway Spruce in Southern Finland and meteorological variables: monthly mean temperature (Temp.), precipitation sums (Prec.), and standardized precipitation evapotranspiration index (SPEI) for the 30-year moving intervals during the 1954–2017 period. The thick line represents significant correlations at $\alpha = 0.05$. Only the meteorological variables showing explicit changes or stationarity in correlations are shown for clarity. Note that the displayed variables differ among the panels; Figure S5, Bootstrapped Pearson correlation coefficients between residual chronologies of tree-ring width of the studied open-pollinated stands of Norway Spruce in Estonia and meteorological variables: monthly mean temperature (Temp.), precipitation sums (Prec.), and standardized precipitation evapotranspiration index (SPEI) for the 30-year moving intervals during the 1954–2017 period. The thick line represents significant correlations at $\alpha = 0.05$. Only the meteorological variables showing explicit changes or stationarity in correlations are shown for clarity. Note that the displayed variables differ among the panels; Figure S6, Bootstrapped Pearson correlation coefficients between residual chronologies of tree-ring width of the studied open-pollinated stands of Norway Spruce in Latvia and meteorological variables: monthly mean temperature (Temp.), precipitation sums (Prec.), and standardized precipitation evapotranspiration index (SPEI) for the 30-year moving intervals during the 1954–2017 period. The thick line represents significant correlations at $\alpha = 0.05$. Only the meteorological variables showing explicit changes or stationarity in correlations are shown for clarity. Note that the displayed variables differ among the panels; Figure S7, Bootstrapped Pearson correlation coefficients between residual chronologies of tree-ring width of the studied open-pollinated stands of Norway Spruce in Lithuania and meteorological variables: monthly mean temperature (Temp.), precipitation sums (Prec.), and standardized precipitation evapotranspiration index (SPEI) for the 30-year moving intervals during the 1954–2017 period. The thick line represents significant correlations at $\alpha = 0.05$. Only the meteorological variables showing explicit changes or stationarity in correlations are shown for clarity. Note that the displayed variables differ among the panels; Figure S8, Bootstrapped Pearson correlation coefficients between residual chronologies of tree-ring width of the studied open-pollinated stands of Norway Spruce in Poland and meteorological variables: monthly mean temperature (Temp.), precipitation sums (Prec.), and standardized precipitation evapotranspiration index (SPEI) for the 30-year moving intervals during the 1954–2017 period. The thick line represents significant correlations at $\alpha = 0.05$. Only the meteorological variables showing explicit changes or stationarity in correlations are shown for clarity. Note that the displayed variables differ among the panels; Figure S9, Bootstrapped Pearson correlation coefficients between residual chronologies of tree-ring width of the studied open-pollinated stands of Norway Spruce in Northern Germany and meteorological variables: monthly mean temperature (Temp.), precipitation sums (Prec.), and standardized precipitation evapotranspiration index (SPEI) for the 30-year moving intervals during the 1954–2017 period. The thick line represents significant correlations at $\alpha = 0.05$.

Only the meteorological variables showing explicit changes or stationarity in correlations are shown for clarity. Note that the displayed variables differ among the panels.

Author Contributions: Conceptualization, R.M. and Ā.J.; methodology, R.M., D.E., and V.S.; software, D.E. and R.M.; validation, D.E., H.G., and T.W.; formal analysis, D.E. and Ā.J.; investigation, O.K., V.S., T.W., and J.K.; resources, R.M. and Ā.J.; data curation, R.M., V.S., and O.K.; writing—original draft preparation, R.M., H.G., and Ā.J.; writing—review and editing, R.M., H.G., Ā.J., T.W., J.K., and V.S.; visualization, R.M.; supervision, Ā.J. and H.G.; project administration, R.M. and Ā.J.; funding acquisition, R.M. and Ā.J. All authors have read and agreed to the published version of the manuscript.

Funding: The study was conducted under the framework of the post-doctoral studies in Latvia ('Plasticity of development and xylogenesis of the native and introduced tree species under changing climate', project No.: 1.1.1.2.VIAA/1/16/108) and research project "Decision support tool for increased forest productivity via efficient climate adjusted transfer of genetic gain" (No. 1.1.1.1/19/A/111) financed by the European Regional Development Fund.

Data Availability Statement: Not applicable.

Acknowledgments: We are grateful to Martin Wilmking for the idea of assessing nonlinearity of regional growth responses. We also acknowledge the technicians who helped during the selection of sites and sampling.

Conflicts of Interest: The authors declare no conflict of interest. The authors declare that they have no known competing financial interests or personal relationships that could have appeared to influence the work reported in this paper.

References

1. Buras, A.; Menzel, A. Projecting Tree Species Composition Changes of European Forests for 2061–2090 Under RCP 4.5 and RCP 8.5 Scenarios. *Front. Plant Sci.* **2019**, *9*, 1986. [CrossRef] [PubMed]
2. Hanewinkel, M.; Cullmann, D.A.; Schelhaas, M.J.; Nabuurs, G.J.; Zimmermann, N.E. Climate change may cause severe loss in the economic value of European forest land. *Nat. Clim. Chang.* **2013**, *3*, 203–207. [CrossRef]
3. Nabuurs, G.-J.; Verkerk, P.J.; Schelhaas, M.-J.; Ramón González Olabarria, J.; Trasobares, A.; Cienciala, E. Climate-Smart Forestry: Mitigation impacts in three European regions. In *From Science to Policy 6*; European Forest Institute: Joensuu, Finland, 2018; p. 32.
4. Yousefpour, R.; Temperli, C.; Bugmann, H.; Elkin, C.; Hanewinkel, M.; Meilby, H.; Jacobsen, J.B.; Thorsen, B.J. Updating beliefs and combining evidence in adaptive forest management under climate change: A case study of Norway spruce (*Picea abies* L. Karst) in the Black Forest, Germany. *J. Environ. Manag.* **2013**, *122*, 56–64. [CrossRef] [PubMed]
5. Lindner, M.; Maroschek, M.; Netherer, S.; Kremer, A.; Barbati, A.; Garcia-Gonzalo, J.; Seidl, R.; Delzon, S.; Corona, P.; Kolström, M.; et al. Climate change impacts, adaptive capacity, and vulnerability of European forest ecosystems. *For. Ecol. Manag.* **2010**, *259*, 698–709. [CrossRef]
6. Thurm, E.A.; Hernandez, L.; Baltensweiler, A.; Ayan, S.; Rasztovits, E.; Bielak, K.; Zlatanov, T.M.; Hladnik, D.; Balic, B.; Freudenschuss, A.; et al. Alternative tree species under climate warming in managed European forests. *For. Ecol. Manag.* **2018**, *430*, 485–497. [CrossRef]
7. Aitken, S.N.; Bemmels, J.B. Time to get moving: Assisted gene flow of forest trees. *Evol. Appl.* **2016**, *9*, 271–290. [CrossRef] [PubMed]
8. Harvey, J.E.; Smiljanić, M.; Scharnweber, T.; Buras, A.; Cedro, A.; Cruz-García, R.; Drobyshev, I.; Janecka, K.; Jansons, Ā.; Kaczka, R.; et al. Tree growth influenced by warming winter climate and summer moisture availability in northern temperate forests. *Glob. Chang. Biol.* **2020**, *26*, 2505–2518. [CrossRef]
9. Taeger, S.; Sparks, T.H.; Menzel, A. Effects of temperature and drought manipulations on seedlings of Scots pine provenances. *Plant. Biol.* **2015**, *17*, 361–372. [CrossRef]
10. Ditmarova, L.; Kurjak, D.; Palmroth, S.; Kmet, J.; Strelcova, K. Physiological responses of Norway spruce (*Picea abies*) seedlings to drought stress. *Tree Physiol.* **2009**, *30*, 205–213. [CrossRef] [PubMed]
11. Matisons, R.; Elferts, D.; Krišāns, O.; Schneck, V.; Gärtner, H.; Bast, A.; Wojda, T.; Kowalczyk, J.; Jansons, Ā. Non-linear regional weather-growth relationships indicate limited adaptability of the eastern Baltic Scots pine. *For. Ecol. Manag.* **2021**, *479*, 118600. [CrossRef]
12. Cavin, L.; Jump, A.S. Highest drought sensitivity and lowest resistance to growth suppression are found in the range core of the tree *Fagus sylvatica* L. not the equatorial range edge. *Glob. Chang. Biol.* **2017**, *23*, 362–379. [CrossRef]
13. Restaino, C.M.; Peterson, D.L.; Littell, J. Increased water deficit decreases Douglas fir growth throughout western US forests. *Proc. Natl. Acad. Sci. USA* **2016**, *113*, 9557–9562. [CrossRef] [PubMed]

14. Wilmking, M.; Maaten-Theunissen, M.; Maaten, E.; Scharnweber, T.; Buras, A.; Biermann, C.; Gurskaya, M.; Hallinger, M.; Lange, J.; Shetti, R.; et al. Global assessment of relationships between climate and tree growth. *Glob. Chang. Biol.* **2020**, *26*, 3212–3220. [CrossRef] [PubMed]
15. Castagneri, D.; Fonti, P.; von Arx, G.; Carrer, M. How does climate influence xylem morphogenesis over the growing season? Insights from long-term intra-ring anatomy in *Picea abies*. *Ann. Bot.* **2017**, *119*, mcw274. [CrossRef]
16. Zhang, Z.; Babst, F.; Bellassen, V.; Frank, D.; Launois, T.; Tan, K.; Ciais, P.; Poulter, B. Converging Climate Sensitivities of European Forests Between Observed Radial Tree Growth and Vegetation Models. *Ecosystems* **2018**, *21*, 410–425. [CrossRef]
17. Heer, K.; Behringer, D.; Piermattei, A.; Bässler, C.; Brandl, R.; Fady, B.; Jehl, H.; Liepelt, S.; Lorch, S.; Piotti, A.; et al. Linking dendroecology and association genetics in natural populations: Stress responses archived in tree rings associate with SNP genotypes in silver fir (*Abies alba* Mill.). *Mol. Ecol.* **2018**, *27*, 1428–1438. [CrossRef]
18. Housset, J.M.; Nadeau, S.; Isabel, N.; Depardieu, C.; Duchesne, I.; Lenz, P.; Girardin, M.P. Tree rings provide a new class of phenotypes for genetic associations that foster insights into adaptation of conifers to climate change. *New Phytol.* **2018**, *218*, 630–645. [CrossRef] [PubMed]
19. McCullough, I.M.; Davis, F.W.; Williams, A.P. A range of possibilities: Assessing geographic variation in climate sensitivity of ponderosa pine using tree rings. *For. Ecol. Manag.* **2017**, *402*, 223–233. [CrossRef]
20. Shi, F.; Yang, B.; Linderholm, H.W.; Seftigen, K.; Yang, F.; Yin, Q.; Shao, X.; Guo, Z. Ensemble standardization constraints on the influence of the tree growth trends in dendroclimatology. *Clim. Dyn.* **2020**, *54*, 3387–3404. [CrossRef]
21. Sullivan, P.F.; Pattison, R.R.; Brownlee, A.H.; Cahoon, S.M.P.; Hollingsworth, T.N. Effect of tree-ring detrending method on apparent growth trends of black and white spruce in interior Alaska. *Environ. Res. Lett.* **2016**, *11*, 114007. [CrossRef]
22. Tei, S.; Sugimoto, A.; Yonenobu, H.; Matsuura, Y.; Osawa, A.; Sato, H.; Fujinuma, J.; Maximov, T. Tree-ring analysis and modeling approaches yield contrary response of circumboreal forest productivity to climate change. *Glob. Chang. Biol.* **2017**, *23*, 5179–5188. [CrossRef]
23. Fei, S.; Desprez, J.M.; Potter, K.M.; Jo, I.; Knott, J.A.; Oswalt, C.M. Divergence of species responses to climate change. *Sci. Adv.* **2017**, *3*, e1603055. [CrossRef]
24. Konter, O.; Büntgen, U.; Carrer, M.; Timonen, M.; Esper, J. Climate signal age effects in boreal tree-rings: Lessons to be learned for paleoclimatic reconstructions. *Quat. Sci. Rev.* **2016**, *142*, 164–172. [CrossRef]
25. Hofgaard, A.; Ols, C.; Drobyshev, I.; Kirchhefer, A.J.; Sandberg, S.; Söderström, L. Non-stationary Response of Tree Growth to Climate Trends Along the Arctic Margin. *Ecosystems* **2019**, *22*, 434–451. [CrossRef]
26. Billings, S.A.; Glaser, S.M.; Boone, A.S.; Stephen, F.M. Nonlinear tree growth dynamics predict resilience to disturbance. *Ecosphere* **2015**, *6*, art242. [CrossRef]
27. Lloyd, A.H.; Duffy, P.A.; Mann, D.H. Nonlinear responses of white spruce growth to climate variability in interior Alaska. *Can. J. For. Res.* **2013**, *43*, 331–343. [CrossRef]
28. Matisons, R.; Puriņa, L.; Adamovičs, A.; Robalte, L.; Jansons, Ā. European beech in its northeasternmost stands in Europe: Varying climate-growth relationships among generations and diameter classes. *Dendrochronologia* **2017**, *45*, 123–131. [CrossRef]
29. Ohse, B.; Ohse, B.; Jansen, F.; Wilmking, M. Do limiting factors at Alaskan treelines shift with climatic regimes? *Environ. Res. Lett.* **2012**, *7*, 15505. [CrossRef]
30. Valladares, F.; Matesanz, S.; Guilhaumon, F.; Araújo, M.B.; Balaguer, L.; Benito-Garzón, M.; Cornwell, W.; Gianoli, E.; Kleunen, M.; Naya, D.E.; et al. The effects of phenotypic plasticity and local adaptation on forecasts of species range shifts under climate change. *Ecol. Lett.* **2014**, *17*, 1351–1364. [CrossRef]
31. Booth, T.H. Estimating potential range and hence climatic adaptability in selected tree species. *For. Ecol. Manag.* **2016**, *366*, 175–183. [CrossRef]
32. Seddon, A.W.R.; Macias-Fauria, M.; Long, P.R.; Benz, D.; Willis, K.J. Sensitivity of global terrestrial ecosystems to climate variability. *Nature* **2016**, *531*, 229–232. [CrossRef]
33. Nabais, C.; Hansen, J.K.; David-Schwartz, R.; Klisz, M.; López, R.; Rozenberg, P. The effect of climate on wood density: What provenance trials tell us? *For. Ecol. Manag.* **2018**, *408*, 148–156. [CrossRef]
34. Chauvin, T.; Cochard, H.; Segura, V.; Rozenberg, P. Native-source climate determines the Douglas-fir potential of adaptation to drought. *For. Ecol. Manag.* **2019**, *444*, 9–20. [CrossRef]
35. Moran, E.; Lauder, J.; Musser, C.; Stathos, A.; Shu, M. The genetics of drought tolerance in conifers. *New Phytol.* **2017**, *216*, 1034–1048. [CrossRef] [PubMed]
36. Klisz, M.; Buras, A.; Sass-Klaassen, U.; Puchałka, R.; Koprowski, M.; Ukalska, J. Limitations at the Limit? Diminishing of Genetic Effects in Norway Spruce Provenance Trials. *Front. Plant. Sci.* **2019**, *10*, 306. [CrossRef] [PubMed]
37. Trouillier, M.; van der Maaten-Theunissen, M.; Scharnweber, T.; Würth, D.; Burger, A.; Schnittler, M.; Wilmking, M. Size matters—a comparison of three methods to assess age- and size-dependent climate sensitivity of trees. *Trees Struct. Funct.* **2019**, *33*, 183–192. [CrossRef]
38. Wu, G.; Xu, G.; Chen, T.; Liu, X.; Zhang, Y.; An, W.; Wang, W.; Fang, Z.A.; Yu, S. Age-dependent tree-ring growth responses of Schrenk spruce (*Picea schrenkiana*) to climate—A case study in the Tianshan Mountain, China. *Dendrochronologia* **2013**, *31*, 318–326. [CrossRef]

39. Cuny, H.E.; Rathgeber, C.B.K.; Frank, D.; Fonti, P.; Makinen, H.; Prislan, P.; Rossi, S.; Del Castillo, E.M.; Campelo, F.; Vavrčík, H.; et al. Woody biomass production lags stem-girth increase by over one month in coniferous forests. *Nat. Plants* **2015**, *1*, 1–6. [CrossRef]
40. Cuny, H.E.; Fonti, P.; Rathgeber, C.B.K.; Arx, G.; Peters, R.L.; Frank, D.C. Couplings in cell differentiation kinetics mitigate air temperature influence on conifer wood anatomy. *Plant. Cell Environ.* **2019**, *42*, 1222–1232. [CrossRef]
41. Friedrichs, D.A.; Buntgen, U.; Frank, D.C.; Esper, J.; Neuwirth, B.; Loffler, J. Complex climate controls on 20th century oak growth in Central-West Germany. *Tree Physiol.* **2009**, *29*, 39–51. [CrossRef] [PubMed]
42. Wang, T.; O'Neill, G.A.; Aitken, S.N. Integrating environmental and genetic effects to predict responses of tree populations to climate. *Ecol. Appl.* **2010**, *20*, 153–163. [CrossRef] [PubMed]
43. Parkatti, V.P.; Assmuth, A.; Rämö, J.; Tahvonen, O. Economics of boreal conifer species in continuous cover and rotation forestry. *For. Policy Econ.* **2019**, *100*, 55–67. [CrossRef]
44. Vitali, V.; Büntgen, U.; Bauhus, J. Silver fir and Douglas fir are more tolerant to extreme droughts than Norway spruce in south-western Germany. *Glob. Chang. Biol.* **2017**, *23*, 5108–5119. [CrossRef] [PubMed]
45. Niinimäki, S.; Tahvonen, O.; Mäkelä, A.; Linkosalo, T. On the economics of Norway spruce stands and carbon storage. *Can. J. For. Res.* **2013**, *43*, 637–648. [CrossRef]
46. Netherer, S.; Panassiti, B.; Pennerstorfer, J.; Matthews, B. Acute Drought Is an Important Driver of Bark Beetle Infestation in Austrian Norway Spruce Stands. *Front. For. Glob. Chang.* **2019**, *2*, 39. [CrossRef]
47. Jönsson, A.M.; Appelberg, G.; Harding, S.; Bärring, L. Spatio-temporal impact of climate change on the activity and voltinism of the spruce bark beetle, *Ips typographus*. *Glob. Chang. Biol.* **2009**, *15*, 486–499. [CrossRef]
48. Seidl, R.; Rammer, W.; Jäger, D.; Lexer, M.J. Impact of bark beetle (*Ips typographus* L.) disturbance on timber production and carbon sequestration in different management strategies under climate change. *For. Ecol. Manag.* **2008**, *256*, 209–220. [CrossRef]
49. Hlásny, T.; Barka, I.; Roessiger, J.; Kulla, L.; Trombik, J.; Sarvašová, Z.; Bucha, T.; Kovalčík, M.; Čihák, T. Conversion of Norway spruce forests in the face of climate change: A case study in Central Europe. *Eur. J. For. Res.* **2017**, *136*, 1013–1028. [CrossRef]
50. Skrøppa, T. *Picea abies—Technical Guidelines for Genetic Conservation and Use for Norway Spruce*; Norwegian Forest Research Institute: Ås, Norway, 2003; p. 6.
51. Sedmáková, D.; Sedmák, R.; Bosela, M.; Ježík, M.; Blaženec, M.; Hlásny, T.; Marušák, R. Growth-climate responses indicate shifts in the competitive ability of European beech and Norway spruce under recent climate warming in East-Central Europe. *Dendrochronologia* **2019**, *54*, 37–48. [CrossRef]
52. Mäkinen, H.; Nöjd, P.; Kahle, H.P.; Neumann, U.; Tveite, B.; Mielikäinen, K.; Röhle, H.; Spiecker, H. Radial growth variation of Norway spruce (*Picea abies* (L.) Karst.) across latitudinal and altitudinal gradients in central and northern Europe. *For. Ecol. Manag.* **2002**, *171*, 243–259. [CrossRef]
53. Weigel, R.; Muffler, L.; Klisz, M.; Kreyling, J.; Van Der Maaten-Theunissen, M.; Wilmking, M.; Van Der Maaten, E. Winter matters: Sensitivity to winter climate and cold events increases towards the cold distribution margin of European beech (*Fagus sylvatica* L.). *J. Biogeogr.* **2018**, *45*, 2779–2790. [CrossRef]
54. Harris, I.; Jones, P.D.; Osborn, T.J.; Lister, D.H. Updated high-resolution grids of monthly climatic observations—the CRU TS3.10 Dataset. *Int. J. Climatol.* **2014**, *34*, 623–642. [CrossRef]
55. Trajkovic, S. Temperature-Based Approaches for Estimating Reference Evapotranspiration. *J. Irrig. Drain. Eng.* **2005**, *131*, 316–323. [CrossRef]
56. Hartmann, D.L.; Klein Tank, A.M.G.; Rusticucci, M.; Alexander, L.V.; Brönnimann, S.; Charabi, Y.A.R.; Dentener, F.J.; Dlugokencky, E.J.; Easterling, D.R.; Kaplan, A.; et al. Observations: Atmosphere and surface. In *Climate Change 2013 the Physical Science Basis: Working Group I Contribution to the Fifth Assessment Report of the Intergovernmental Panel on Climate Change*; Cambridge University Press: Cambridge, UK, 2013; Volume 9781107057999, pp. 159–254. ISBN 9781107415324.
57. Gärtner, H.; Nievergelt, D. The core-microtome: A new tool for surface preparation on cores and time series analysis of varying cell parameters. *Dendrochronologia* **2010**, *28*, 85–92. [CrossRef]
58. Bunn, A.G. A dendrochronology program library in R (dplR). *Dendrochronologia* **2008**, *26*, 115–124. [CrossRef]
59. Wigley, T.M.L.; Briffa, K.R.; Jones, P.D. On the average value of correlated time series with applications in dendroclimatology and hydrometeorology. *J. Clim. Appl. Meteorol.* **1984**, *23*, 201–213. [CrossRef]
60. Von Arx, G.; Arzac, A.; Fonti, P.; Frank, D.; Zweifel, R.; Rigling, A.; Galiano, L.; Gessler, A.; Olano, J.M. Responses of sapwood ray parenchyma and non-structural carbohydrates of Pinus sylvestris to drought and long-term irrigation. *Funct. Ecol.* **2017**, *31*, 1371–1382. [CrossRef]
61. Way, D.A.; Oren, R. Differential responses to changes in growth temperature between trees from different functional groups and biomes: A review and synthesis of data. *Tree Physiol.* **2010**, *30*, 669–688. [CrossRef]
62. Zang, C.; Biondi, F. Dendroclimatic calibration in R: The bootRes package for response and correlation function analysis. *Dendrochronologia* **2013**, *31*, 68–74. [CrossRef]
63. Vicente-Serrano, S.M.; Beguería, S.; López-Moreno, J.I. A multiscalar drought index sensitive to global warming: The standardized precipitation evapotranspiration index. *J. Clim.* **2010**, *23*, 1696–1718. [CrossRef]
64. Sass-Klaassen, U.; Fonti, P.; Cherubini, P.; Gričar, J.; Robert, E.M.R.; Steppe, K.; Bräuning, A. A Tree-Centered Approach to Assess Impacts of Extreme Climatic Events on Forests. *Front. Plant. Sci.* **2016**, *7*, 1069. [CrossRef] [PubMed]

65. Wood, S.N. Fast stable restricted maximum likelihood and marginal likelihood estimation of semiparametric generalized linear models. *J. R. Stat. Soc. Ser. B* **2011**, *73*, 3–36. [CrossRef]
66. R Core Team R. *A Language and Environment for Statistical Computing*; R Foundation for Statistical Computing: Vienna, Austria. Available online: http://www.r-project.org/ (accessed on 5 December 2019).
67. Fox, J.; Weisberg, S. An R Companion to Applied Regression. Available online: https://socialsciences.mcmaster.ca/jfox/Books/Companion/ (accessed on 12 March 2021).
68. Mina, M.; Martin-Benito, D.; Bugmann, H.; Cailleret, M. Forward modeling of tree-ring width improves simulation of forest growth responses to drought. *Agric. For. Meteorol.* **2016**, *221*, 13–33. [CrossRef]
69. Potokina, E.K.; Kiseleva, A.A.; Nikolaeva, M.A.; Ivanov, S.A.; Ulianich, P.S.; Potokin, A.F. Analysis of the polymorphism of organelle DNA to elucidate the phylogeography of Norway spruce in the East European Plain. *Russ. J. Genet. Appl. Res.* **2015**, *5*, 430–439. [CrossRef]
70. Loehle, C. Height growth rate tradeoffs determine northern and southern range limits for trees. *J. Biogeogr.* **1998**, *25*, 735–742. [CrossRef]
71. Carrer, M.; Urbinati, C. Long-term change in the sensitivity of tree-ring growth to climate forcing in *Larix decidua*. *New Phytol.* **2006**, *170*, 861–872. [CrossRef] [PubMed]
72. Zhang, T.; Zhang, R.; Jiang, S.; Bagila, M.; Ainur, U.; Yu, S. On the 'Divergence Problem' in the Alatau Mountains, Central Asia: A Study of the Responses of Schrenk Spruce Tree-Ring Width to Climate under the Recent Warming and Wetting Trend. *Atmosphere* **2019**, *10*, 473. [CrossRef]
73. Allen, K.J.; Villalba, R.; Lavergne, A.; Palmer, J.G.; Cook, E.C.; Fenwick, P.; Drew, D.M.; Turney, C.S.M.; Baker, P.J. A comparison of some simple methods used to detect unstable temperature responses in tree-ring chronologies. *Dendrochronologia* **2018**, *48*, 52–73. [CrossRef]
74. D'Arrigo, R.; Wilson, R.; Liepert, B.; Cherubini, P. On the "Divergence Problem" in Northern Forests: A review of the tree-ring evidence and possible causes. *Glob. Planet. Chang.* **2008**, *60*, 289–305. [CrossRef]
75. Yang, X.; Tang, J.; Mustard, J.F.; Lee, J.-E.; Rossini, M.; Joiner, J.; Munger, J.W.; Kornfeld, A.; Richardson, A.D. Solar-induced chlorophyll fluorescence that correlates with canopy photosynthesis on diurnal and seasonal scales in a temperate deciduous forest. *Geophys. Res. Lett.* **2015**, *42*, 2977–2987. [CrossRef]
76. Jyske, T.; Mäkinen, H.; Kalliokoski, T.; Nöjd, P. Intra-annual tracheid production of Norway spruce and Scots pine across a latitudinal gradient in Finland. *Agric. For. Meteorol.* **2014**, *194*, 241–254. [CrossRef]
77. Carrer, M.; Nola, P.; Motta, R.; Urbinati, C. Contrasting tree-ring growth to climate responses of Abies alba toward the southern limit of its distribution area. *Oikos* **2010**, *119*, 1515–1525. [CrossRef]
78. Pallardy, S.G. *Physiology of Woody Plants*, 3rd ed.; Elsevier: London, UK, 2008.
79. Strand, M.; Löfvenius, M.O.; Bergsten, U.; Lundmark, T.; Rosvall, O. Height growth of planted conifer seedlings in relation to solar radiation and position in Scots pine shelterwood. In *Forest Ecology and Management*; Elsevier: Amsterdam, The Netherlands, 2006; Volume 224, pp. 258–265.
80. Tei, S.; Sugimoto, A. Time lag and negative responses of forest greenness and tree growth to warming over circumboreal forests. *Glob. Chang. Biol.* **2018**, *24*, 4225–4237. [CrossRef] [PubMed]
81. Hacket-Pain, A.; Ascoli, D.; Berretti, R.; Mencuccini, M.; Motta, R.; Nola, P.; Piussi, P.; Ruffinatto, F.; Vacchiano, G. Temperature and masting control Norway spruce growth, but with high individual tree variability. *For. Ecol. Manag.* **2019**, *438*, 142–150. [CrossRef]
82. Heide, O.M. Growth and Dormancy in Norway Spruce Ecotypes. II. After-effects of Photoperiod and Temperature on Growth and Development in Subsequent Years. *Physiol. Plant.* **1974**, *31*, 131–139. [CrossRef]
83. Pearce, R. Plant Freezing and Damage. *Ann. Bot.* **2001**, *87*, 417–424. [CrossRef]
84. Tierney, G.L.; Fahey, T.J.; Groffman, P.M.; Hardy, J.P.; Fitzhugh, R.D.; Driscoll, C.T. Soil freezing alters fine root dynamics in a northern hardwood forest. *Biogeochemistry* **2001**, *56*, 175–190. [CrossRef]
85. Hansen, J.; Beck, E. Seasonal changes in the utilization and turnover of assimilation products in 8-year-old Scots pine (*Pinus sylvestris* L.) trees. *Trees* **1994**, *8*, 172–182. [CrossRef]
86. Beck, E.H.; Heim, R.; Hansen, J. Plant resistance to cold stress: Mechanisms and environmental signals triggering frost hardening and dehardening. *J. Biosci.* **2004**, *29*, 449–459. [CrossRef] [PubMed]
87. Ogren, E. Relationship between temperature, respiratory loss of sugar and premature dehardening in dormant Scots pine seedlings. *Tree Physiol.* **1997**, *17*, 47–51. [CrossRef]
88. Burt, T.P.; Pinay, G.; Matheson, F.E.; Haycock, N.E.; Butturini, A.; Clement, J.C.; Danielescu, S.; Dowrick, D.J.; Hefting, M.M.; Hillbricht-Ilkowska, A.; et al. Water table fluctuations in the riparian zone: Comparative results from a pan-European experiment. *J. Hydrol.* **2002**, *265*, 129–148. [CrossRef]